Size dependence of the pressure-induced γ to α structural transition in iron oxide nanocrystals

S.M. Clark*[1], S.G. Prilliman*[2], C.K. Erdonmez[2], J. Rockenberger[2], D.J. Zaziski[2], J. Kwong[2], and A.P. Alivisatos[2]

[1]Advanced Light Source, Lawrence Berkeley National Laboratory, MS6R2100, Berkeley, CA 94720
[2]Department of Chemistry, University of California, Berkeley, CA 94720 and Materials Science Division, Lawrence Berkeley National Laboratory, Berkeley, CA 94720

*These authors contributed equally

The size trend for the pressure-induced γ-Fe_2O_3 (maghemite) to α-Fe_2O_3 (hematite) structural phase transition in nanocrystals has been observed. The transition pressure was found to increase with decreasing nanocrystal size: 7 nm nanocrystals transformed at 27GPa, 5 nm at 34GPa and 3 nm at 37GPa. Comparison with literature data on larger γ-Fe_2O_3 nanocrystals suggests that the effect saturates at a particle size of roughly 7 nm, indicating a structural or electronic transition at that size. Annealing of a bulk sample of γ-Fe_2O_3 was found to greatly reduce the transition pressure from 35 to 24GPa. The bulk modulus was determined to be ~ 260GPa for 7 nm nanocrystals of γ-Fe_2O_3, which is significantly higher than for the value of 190GPa we measured for bulk samples. For α-Fe_2O_3, the bulk moduli for 7 nm nanocrystals and bulk were almost the same within error. The bulk modulus for the γ phase was found to decrease with decreasing particle size between 10 and 3.2 nm particle size. Values for the ambient pressure molar volume were found within 1% to be: 33.0 cc/mol for bulk γ-Fe_2O_3, 32.8 cc/mol for 7 nm diameter γ-Fe_2O_3 nanocrystals, 30.7 cc/mol for bulk α-Fe_2O_3 and 30.6 cc/mol for α-Fe_2O_3 nanocrystals. As the size of γ-Fe_2O_3 nanocrystals is decreased, the onset of the softening of the lattice precedes the onset of the change in transition pressure. The change in transition pressure is argued to be a result of the lattice softening.

PACS numbers
61.10.-I – X-ray diffraction and scattering
62.50.+p – High-pressure and shock wave effects in solids and liquids
64.70.Kb – Solid-solid transitions

I. INTRODUCTION

The properties of nanoscale materials can be quite different from bulk[1]. Some properties have been found to vary continuously with particle size, the most famous example being the reduction in melting temperature in smaller sizes[2]. The reduction is driven by the fact that the liquid generally has a lower surface energy than the solid, and is observed almost universally (although

theoretically it is possible for the melting of an embedded nanocrystal to increase in smaller sizes, if the surface energy of the solid-solid interface is lower than the solid-liquid surface energy). For some time now we have been interested in determining if there is a comparable trend with size in pressure induced solid-solid transformations to denser structures. The earliest, and still most comprehensive, study of a pressure-induced phase transition used well characterized nanocrystals of CdSe[3,4] and demonstrated an increase of transition pressure with decreasing nanocrystal size. Enhancement of transition pressure in different nanoscale materials were reported in a large number of following studies. These include the anatase form of TiO_2[5-7], the rutile form of TiO_2[8], ZrO_2[9], PbS[10,11], ZnS[12,13], Si[14], ZnO[15], GaAs[16], WO_3[17] and $CoFe_2O_4$[18]. The increase in transition pressure may arise because the nanocrystals change shape upon structural transformation, creating high energy surfaces in the denser phase. In this picture, the shape change occurs when there is only one nucleation event per nanocrystal, and a pathway that leads from one structure to another.

It is clearly possible for the transition to be lower in smaller nanocrystals, for both thermodynamic and kinetic reasons. There is one case, the pressure-induced transition from γ-Fe_2O_3 to α-Fe_2O_3[19-21], where early evidence has suggested that a pressure induced solid-solid transition is indeed reduced in nanocrystals, compared to the bulk. The study of Jiang et al.[19] found a transition pressure of 27GPa for 9 nm nanocrystals, the Zhao et al. study[20] found a value of 25-30GPa for 10 nm nanocrystals and the Wang and Saxena study[21] found a transition pressure of 26.6GPa for 25 nm nanocrystals. This compares with reported values of 35GPa for bulk material[19,21]. The study of Wang and Saxena[21] went on to study the α-Fe_2O_3 to perovskite structure transition at higher pressure and found no difference in transition pressure to that of bulk material. One significant difficulty arises from the fact that transitions that involve a large volume change usually exhibit significant hysteresis, so that it can be difficult to distinguish between kinetically controlled upstroke observations and the thermodynamic transition points. Examples where this has been an issue includes: SnO_2[22], α-Fe[23] and CeO_2[24]. A further study on the iron oxide system, using an extended range of nanocrystal sizes below 9nm, may prove helpful in determining whether there is a decrease in transition pressure with decreasing nanocrystal size. Here, we present the results of a study of the γ-Fe_2O_3 to α-Fe_2O_3 upstroke transition pressures in well-defined, isolated nanocrystals, dispersed in a soft matrix (not a polycrystalline powder) for a range of nanocrystal sizes and for bulk material. Combining our data with the literature data allows us to more definitively establish a trend with size, not only for the transition pressure, but also for the bulk modulus.

II. EXPERIMENTAL

Samples of γ-Fe_2O_3 nanocrystals were synthesized by a variation of a published method[25]. Briefly, cupferrone, an oxygen terminated bidentate chealating agent, was complexed with Fe^{3+} in aqueous solution. The product was purified, dried and dissolved in hexadecylamine under argon. When the solution was heated to approximately 200°C, iron cupferronate was decomposed, producing γ-Fe_2O_3 nanocrystals. Samples were maintained at 270°C for 5 to 40 minutes, during which time the particles grew in size. By quenching the reaction at different times, nanocrystals of 3.2 nm, 5.7 nm and 7.2 nm average diameter were obtained. The final washed particles retained a monolayer coating of hexadecylamine, making them soluble in non-polar solvents. Samples were evaluated by transmission electron microscopy and x-ray

diffraction, both of which yield approximately the same size for each sample, indicating that each nanocrystal is composed of a single crystalline domain. Size distributions for each sample were approximately ± 15%. Bulk γ-Fe_2O_3 powder (99.9%) was purchased from Aldrich Inc. This was divided into three aliquots. The first was left as delivered, the second was annealed for five days, and the third was annealed for two months. Annealing was conducted at 140°C under vacuum, well below the ~300°C necessary to nucleate α-Fe_2O_3. Phase purity was confirmed by ambient pressure x-ray diffraction. High-pressure measurements were made on all three samples.

High pressures were generated using a diamond anvil cell (DAC), type WCME, supplied by Diacell Products Ltd. Diamonds with 300 μm culet diameter were used with spring steel gaskets with 150 μm holes. Nanocrystals were redissolved in ethylcyclohexane and bulk samples were dispersed in the same solvent. The pressure was measured using the ruby fluorescence method[26]. Each sample was pressurized up to 40GPa in 2-5GPa pressure increments. X-ray powder diffraction patterns were collected at each pressure. These data were collected on beamline 7.3.3 at the Advanced Light Source, Lawrence Berkeley National Laboratory, Berkeley, CA. This beamline is optimised for DAC studies using angle-dispersive diffraction[27,28]. The synchrotron beam was focused to a size of 50 x 120 μm at the sample. The optimal wavelength for these measurements on this beamline was found to be 1.117 Å, which was used throughout. Two dimensional diffraction patterns were collected using a Mar345 imaging plate detector system (Mar Research, Evanston, IL). Diffraction patterns were taken, with exposure times of 25 minutes, at regular intervals of approximately one every 50 minutes in order to minimize kinetic effects. The sample-to-detector distance was calibrated using LaB_6 and Al_2O_3 as diffraction standards. The system accuracy was found to be approximately 0.01 degrees in 2θ, or 0.001 Å in d-spacing. Two-dimensional diffraction patterns were radially integrated using the program Fit2D[29], to obtain one-dimensional patterns. Voigt peak shape functions were fitted to these patterns in order to determine diffraction peak positions and widths. All measurements were made at room temperature.

III. RESULTS

Fig. 1 shows selected diffraction patterns at a number of pressures for the briefly annealed bulk γ-Fe_2O_3 sample (a) and for 7.2 nm γ-Fe_2O_3 nanocrystals (b). The peaks of the nanocrystal samples are Debye-Scherrer broadened relative to the bulk as expected[30]. For both nanocrystal and bulk samples, only the γ phase was present at low pressures. As pressure was increased, peaks associated with the α phase began to appear. Finally, at even higher pressures, pure α phase was obtained. When quenched to atmospheric pressure, both bulk and nanocrystal samples retained the α structure. The peak widths of the narrowest peaks of the bulk samples increased from 0.3° to 0.5° across the transition. The peak widths of both α-Fe_2O_3 nanocrystals and γ-Fe_2O_3 nanocrystals were both found to be about 1.0° throughout the measurements.

Because some peaks were less intense and broader in the α phase, it was difficult to accurately determine the phase percentages at a given pressure. Following the method of Jiang et al.[19], we quantified the transition progress by plotting the ratio of the integral intensities of the γ-Fe_2O_3 (311) and γ-Fe_2O_3 (220) diffraction peaks as a function of pressure. The γ-Fe_2O_3 (311) coincides

closely with the α-Fe_2O_3 (110), while the γ-Fe_2O_3 (220) has no coincident peak in the α-Fe_2O_3 pattern. As the transition proceeds, the I^{220}/I^{311} ratio increases from its pure γ-Fe_2O_3 value of approximately 3.0. The result of this analysis is presented in Fig. 2(a) for nanocrystal samples with diameters of 3.2 nm, 4.9 nm, and 7.2 nm. We observe that for decreasing nanocrystal diameters, the rise in the I^{220}/I^{311} ratio is shifted to higher pressures. This allows us to estimate the transition pressures as: 27GPa for 7.2 nm diameter nanocrystals, 34GPa for 4.9 nm and 37GPa for 3.2 nm. For bulk samples (Fig. 2b) the observed transition pressure decreases with increasing annealing time.

In addition to transition pressures, we determined from our data bulk moduli and ambient pressure volumes for bulk γ-Fe_2O_3, bulk α-Fe_2O_3 formed by phase transition from bulk γ-Fe_2O_3, 7 nm nanocrystals of γ-Fe_2O_3 and α-Fe_2O_3 nanocrystals formed by phase transition from 7 nm nanocrystals of γ-Fe_2O_3 (Table 1). The unit cell volume as a function of pressure for nanocrystals (open symbols) and bulk (filled symbols) is shown for γ-Fe_2O_3 (triangles) and α-Fe_2O_3 (squares) in Fig. 3. The values in Table 1 were obtained by fitting the Birch equation[31] to our data with the pressure derivative of the bulk modulus set to a value of 4 after Jiang et al.[19]. The Birch equation fits are also shown graphically in Fig. 3. For fitting purposes, only data from diffraction patterns clearly showing a single phase was used in order to avoid errors due to overlapping γ-Fe_2O_3 and α-Fe_2O_3 peaks. Volumes for bulk α-Fe_2O_3 formed from the variously annealed bulk γ-Fe_2O_3 samples were found to be indistinguishable. Therefore, these volumes were combined before determining the values in Table 1. The percentage volume change at the mid point of the transition was found to be about 10%.

Table 1. Bulk moduli and molar volume at ambient pressure obtained by fitting the Birch equation to our data.

Sample	Bulk Modulus (GPa)	Molar Vol. at Ambient Pressure (cc/mol)
Bulk γ-Fe_2O_3	190 ± 6	33.0 ± 0.2
7 nm γ-Fe_2O_3	262 ± 6	32.8 ± 0.2
Bulk α-Fe_2O_3	300 ± 30	30.7 ± 0.3
7 nm α-Fe_2O_3	336 ± 5	30.6 ± 0.1

IV. DISCUSSION

Our data show that the upstroke transition pressure for the γ-Fe_2O_3 to α-Fe_2O_3 phase transition for nanocrystal samples increases as the nanocrystal size decreases for nanocrystals in the range 3.2 to 7.2 nm. The transition pressure of 27GPa that we have determined for the 7.2 nm diameter nanocrystals is, within error, the same as the values of 27GPa determined by Jiang et al.[19] for 9 nm diameter nanocrystals, 26.6GPa determined by Wang and Saxena[21] for 25 nm nanocrystals and 24 ± 2GPa determined for our annealed bulk sample (Fig. 4). It seems that the effect of particle size on the transition pressure saturates at about 7 nm particle size with all larger sizes giving the same value as a fully annealed bulk sample. One might argue that pressure annealing

of aggregated particles has led to grain growth and production of bulk from nanocrystals and hence bulk measurements from what were initially nanocrystals. This seems unlikely since no sharpening of the diffraction peak widths was observed in our measurements or reported in the literature measurements. The increase in the transition pressure at small particle sizes might be attributed to an increased contribution from an unfavorable surface energy component to the total energy or the crossing of a critical size for a structural transition. We would expect the former of these mechanisms to lead to a more gradual increase in the transition pressure than actually observed. The sudden increase in transition pressure as particle size drops below 7 nm seems more in keeping with a sharp change in nanocrystal properties around that size.

The variation of the transition pressure for the bulk sample with annealing time is not surprising. Maghemite has a cation deficient spinel structure which may be represented as: $Fe_8[Fe_{40/3}[]_{8/3}]O_{32}$ where [] denotes vacancy. Eight Fe^{3+} atoms occupy tetrahedral sites while the remainder occupies octahedral sites. The vacancies may be ordered or disordered or partially occupied by impurity atoms. This allows a certain amount of variability of the crystal structure and microstructure depending on sample preparation and history. This is manifested in, for example, the thermal transition from γ-Fe_2O_3 to α-Fe_2O_3 that has been found to depend strongly on sample preparation[32]. The important point is that annealing the bulk γ sample reduced the transition pressure to a limiting value similar to that found for nanocrystals larger than 7nm.

The value we determined for the bulk modulus of bulk γ-Fe_2O_3, 190 ± 6GPa, agrees within error with the value of 203 ± 10GPa found by Jiang et al.[19] The value of the bulk modulus we found for γ-Fe_2O_3 nanocrystals, 262 ± 6GPa, is significantly lower than the value of 305 ± 15GPa found by Jiang et al.[19] and 375 ± 9GPa found by Zhao et al.[20] Due to the wide peak widths and low intensity of the diffraction profiles from very small nanocrystals we were unable to determine a reliable bulk modulus from our 3.2 or 4.9 nm diameter samples. When we combine all of our nanoparticle data together we obtain a bulk modulus of 211 ± 15GPa which we can use as an indication of the relative change in bulk modulus with particle size. All of these values are shown in Fig. 5. The bulk modulus clearly increases with increasing nanoparticle size. An increase in bulk modulus with nanoparticle size was also observed for γ -Al_2O_3[33]. These values are also plotted in Fig. 5. The γ-Al_2O_3 bulk modulus is seen to smoothly increase to a value close to that of the bulk value of 254GPa[34]. In contrast the bulk modulus of γ-Fe_2O_3 increases to values in excess of the bulk value of about 200GPa. Presumably, there exists a peak value of the bulk modulus at some particle size between 10 nm and that of the bulk. This decrease in the bulk modulus, or softening of the material, is not easily explained in terms of surface energy or kinetic effects. A more plausible explanation of the softening of bulk in comparison with 10 nm nanocrystals can be given by noting that maghemite produced by thermal oxidation of magnetite is known to possess ordering of cation vacancies within a tetragonal supercell for large (> 200 nm) particles and the absence of this type of ordering of vacancies in fine particles (< 100 nm)[36]. Such a loss of order may explain the increase in bulk modulus between bulk and nanocrystals. Enhanced bulk modulus in nanocrystals has been observed before, for example in ZnS[36], and attributed to increase in disorder.

The value we found for the ambient pressure molar volume of γ-Fe_2O_3, 33.0 cc/mol, is the same, within error, as the value of 32.9cc/mol found both by Jiang et al.[21] and Haul and Schoon[37].

The values we determined for the bulk moduli of both bulk and nanocrystalline α-Fe_2O_3 are higher than those previously reported. Our value of 299 ± 30GPa for bulk α-Fe_2O_3 is larger than the value of 205 ± 5GPa determined by Jiang et al.[19], 231 ± 10GPa determined by Sato and Akimoto[38], 225 ± 4GPa determined by Finger and Hazen[39], 258 ± 6GPa determined by Rozenburg et al.[40] and 206 ± 5GPa by Liu et al.[41]. The bulk modulus of bulk α-Fe_2O_3 does seem to be very sensitive to the pressure transmitting medium and the degree of hydrostaticity[41]. Our use of ethylcyclohexane as the pressure transmitting fluid may have exacerbated this situation. Alternatively, the large variation of compressibility and transition behavior has also been attributed to impurities and crystallization history[39]. Other properties of α-Fe_2O_3 have also been found to depend on the method of sample preparation[42]. So it may be that our method of preparing the bulk α-Fe_2O_3 sample, by pressure-induced transformation from bulk γ-Fe_2O_3 may lead to a sample with a higher bulk modulus. The value we determined for the ambient pressure molar volume of bulk α-Fe_2O_3, 30.7 ± 0.3 agrees, within experimental error, with values of 30.3 to 30.4cc/mol determined previously[19,39,40,42].

V. CONCLUSIONS

The upstroke transition pressure for the γ-Fe_2O_3 to α-Fe_2O_3 phase transition was found to increase with decreasing nanocrystal size below about 7 nm nanocrystal size. Above 7 nm, the nanocrystals were found to transform at a constant pressure, which is the same pressure as determined for an annealed bulk sample. The bulk modulus of nanocrystalline γ-Fe_2O_3 was found to initially increase with crystal size, peaking somewhere between 10 nm and bulk. An explanation for the origin of the elevated transition pressure must await further studies of the kinetics of the transition (rate constants versus temperature, pressure, size); however, the preliminary results presented here do establish the correct size dependent trend.

ACKNOWLEDGEMENTS

We would like to thank Rich Celestre, Alastair Macdowell and Edward Domining for help on beamline 7.2.2. and Raymond Jeanloz for helpful discussions. The Advanced Light Source is supported by the Director, Office of Science, Office of Basic Energy Sciences, Materials Sciences Division, of the U.S. Department of Energy under Contract No. DE-AC03-76SF00098 at Lawrence Berkeley National Laboratory.

References

[1]A.P. Alivisatos, P.F. Barbara, A.W. Castleman, J. Chang, D.A. Dixon, M.L. Klein, G.L. McLendon, J.S. Miller, M.A. Ratner, P.J. Rossky, S.Z. Stuppp and M.E. Thompson, *Adv. Mater*. **10,** 297 (1998).
[2]P. Buffat and J. P. Borel, Physical Review A **13(6)**, 2287 (1976).
[3]S.H. Tolbert and A.P. Alivisatos, *Science* **265,** 373 (1994).
[4]S.H. Tolbert and A.P. Alivisatos, *J. Chem. Phys.,* **102(11),** 4642 (1995).
[5]V. Swarmy, L.S. Dubrovinsky, N.A. Dubrovinskaia, A.S. Simionovici, M. Drakopoulos, V. Dmitriev and H-P. Weber, *Solid State Comm.* **125,** 111 (2003)

[6]Z. Wang and S.K. Saxena, *Solid State Comm.* **118,** 75 (2001)
[7]Z. Wang, S.K. Saxena, V. Pischedda, H.P. Liermann, C.S. Zha, *J. Phys. Condens. Matter*, **31,** 8317 (2001).
[8]J. Staun Olsen, L. Gerward and J.Z. Jiang, *High Pres. Res.* **22,** 385 (2002).
[9]S. Kawasaki, T. Yamanaka, S. Kune and T. Ashida, *Solid State Commun.* **76,** 527 (1990).
[10]S.B. Qadri, J. Yang, B.R. Ratna and E.F. Skelton, *Appl. Phys. Lett.* **69(15),** 2205 (1996).
[11]J.Z. Jiang, L. Gerward, R. Secco, D. Frost, J.S. Olsen and J. Truckenbrodt, *J. App. Phys.* **87(5),** 2658 (2000).
[12]J.Z. Jiang, L. Gerward, D. Frost, R. Secco, J. Peyronneau and J.S. Olsen, *J. App. Phys.* **86(11),** 66088 (1999).
[13]Y. Ji, L. Guo, H. Xu, J. Liu, X. Li, Y. Li, Z. Wu and P. Simon, *Phys. stat. sol. (a)* **198(1)**, 210 (2003).
[14]S.H. Tolbert, A.B. Herhold, L.E. Brus and A.P. Alivisatos, *Phys. Rev. Lett.* **76(23),** 4384 (1996).
[15]J.Z. Jiang, J.S. Olsen, L. Gerward, D. Frost, D. Rubie and J. Peyronneau, *Europhys. Lett.* **50(1),** 48 (2000).
[16]J.Z. Jiang, J. Staun Olsen, L. Gerward and S. Steenstrup, *High Pressure Res.* **22,** 395 (2002).
[17]M. Boulova and G. Lucazeau, *J. Solid State Chem.* **167,** 425 (2002).
[18]Z. Wu, Z. Bao, L. Cao, C. Liu, Q. Li, S. Xie and B.. Zou, *J. Appl. Phys.* **93(12),** 9983 (2003).
[19]J.Z. Jiang, L. Gerward and J.S. Olsen, *Scripta mater*. **44,** 1983 (2001).
[20]J.Z. Jiang, J. Staun Olsen and L. Gerward, *Materials Trans.* **42(8),** 1571 (2001).
[21]Z. Wang, S.K. Saxena, V. Pischedda, H.P. Liermann and C.S. Zha, *Phys. Rev*. **B64,** 012102 (2001).
[22]J.Z. Jiang, J. Staun Olsen, L. Gerward and S. Morup, *Europhys. Lett.* **44(5),** 620 (1998).
[23]J. Zhao, L. Guo, J. Liu, Y. Yang, R. Chen and L. Zhou, *Chin. Phys. Lett*. **17(2),** 126 (2000).
[24]Z. Wang and S.K. Saxena, *Solid State Comm*., **123,** 195 (2002).
[25]J. Rockenberger, E. C. Scher, and A. P. Alivisatos, Journal of the American Chemical Society **121,** 11595 (1999).
[26]M. Eremets, *High Pressure Experimetal Methods*, Oxford University Press, Oxford (1996).
[27]O. Shimomura, K. Takemura, H. Fujihisa, Y. Fujii, Y. Oshishi, T. Kikegawa, T. Amemiya and T. Matsushita, *Rev. Sci. Instrum.,* **63(1),** 967 (1992).
[28]R.J. Nelmes, P.D. Hatton, M.I. McMahon, R.O. Piltz, J. Crain, R.J. Cernik and G. Bushnell-Wye, *Rev. Sci. Instrum.,* **63(1),** 1039 (1992).
[29]A.P Hammersley, S. O. Svensson, M. Hanfland, A. N. Fitch, and D. Häusermann, *High Pressure Research* **14**, 235 (1996).
[30]A Guinier, *X-ray Diffraction in Crystals, Imprefect Crystals and Amorphous Bodies* (Dover, New York, 1963).
[31]F. Birch, J. Appl. Phys. **9,** 279 (1938).
[32]B. Gillot, H. Nouaim, F. Mathieu and A. Rousset, *Min. Chem. And Phys.* **28(4),** 389 (1991).
[33]B. Chen, D. Penwell, L.R. Benedetti, R. Jeanloz and M.B. Kruger, *Phys. Rev. B* **66,** 144101 (2002).

[34]I. Ohno, S. Yamamoto and O.L. Anderson, J. Phys. Chem. Solids, **47,** 1103 (1986).
[35]R.M. Cornell and U. Schwertmann, **Iron Oxides**, VCH, Weinheim, (1996).
[36]B. Gilbert, F. Huang, H. Zhang, G.A. Waychunas, and J.F. Banfield, *Science* **305**, 651-654 (2004).
[37]R. Haul. and Th. Schoon, *Z. Phys. Chem.* **44,** 216 (1939).
[38]Y. Sato and S. Akimoto, *J. Apply. Phys.* **50**, 5285 (1979).
[39]L.W. Finger and R.M. Hazen, *J. Appl. Phys.* **51(10),** 5362 (1980).
[40]G. Kh. Rozenberg, L.S. Dubrovinsky, M.P. Pasternak, O. Naaman, T. Le Bihan and R. Ahuja, *Phys. Rev. B*, **65,** 064112 (2002).
[41]H. Liu, W.A. Caldwell, L.R. Benedetti, W. Panero and R. Jeanloz, *Phys. Chem. Minerals*, **30,** 582 (2003).
[42]E.N. Maslen, V.A. Streltsov, N.R. Streltsova and N. Ishizawa, *Acta Cryst*. **B50,** 435 (1994).
[43]M.R. Gallas and G.J. Piermarini, *J. Am. Ceram. Soc.* **79,** 2917 (1994).
[44]J. Zhao, G.R. Hearne, M. Maaza, F. Laher-Lacour, M.J. Witcomb, T.L. Bihan and M. Mezouar, *J. Appl. Phys.* **90,** 3280 (2001).

Figure captions

FIG. 1. X-ray diffraction patterns of briefly annealed bulk (a) and 7.2 nm diameter nanocrystalline (b) γ-Fe2O3 at various pressures as noted on the figure. The two lowest patterns show each sample entirely in the γ phase. Peaks labeled with diamonds are (in order, left to right), the γ (220), (311), (400), (422) and (511). As pressure is increased, α peaks appear, until at the highest pressure only α is present. Upon recovery to ambient pressure (topmost patterns), the samples retain the α structure. Labeled with asterisks are (left to right), α (102), (104), (110), (113), (024), and (116).

FIG. 2. The ratio of the integrated intensities of the γ(311)/ γ(220) which increases as the transition to α proceeds. The colloidal nanocrystals (a) studied here demonstrate a strong dependence of transition pressure on size. A wide range of transition pressures can be obtained for the bulk (b) depending on how well the samples has been annealed.

FIG. 3. The volume as a function of pressure of bulk (filled triangles, γ; filled squares, α) and nanocrystals (open triangles, γ; open squares α). A strong departure from the P-V curves was observed only for nanocrystals of the γ phase at pressures above 10GPa.

FIG. 4. Variation of transition pressure as a function of nanocrystal size for Fe_2O_3. The diamonds are our data, the square is from Jiang et al.[19], the triangle is from Zhao et al.[20] and the circle is from Wang and Saxena[21]. Our value for the fully annealed bulk sample has been omitted for the sake of clarity, but would be at the same level as the 7 to 25 nm particle sizes just at around 1000nm particle size.

FIG. 5. Variation of bulk modulus with nanocrystal size for γ-Fe_2O_3 and γ-Al_2O_3. Open symbols are for γ-Al_2O_3 and filled symbols for γ-Fe_2O_3. Filled diamonds are our data, the filled square is from Jiang et al.[19], the filled triangle is from Zhao et al.[20], the open diamonds are from Chen at al.[33], the open square from Gallas et al.[43] and the open triangle from Zhao et al.[44]

FIG. 1.

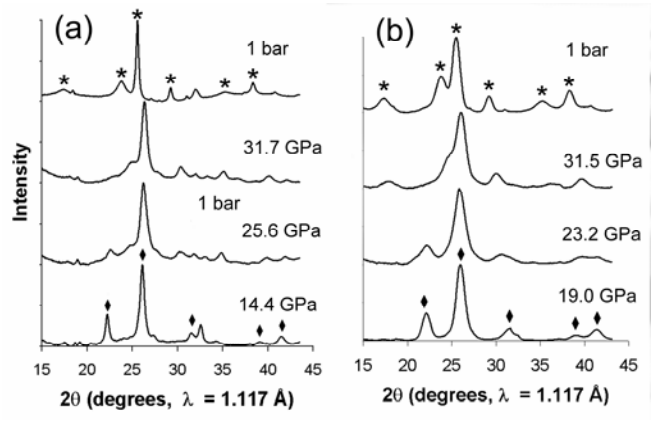
(a)
1 bar
31.7 GPa
1 bar
25.6 GPa
14.4 GPa
Intensity
15 20 25 30 35 40 45
2θ (degrees, λ = 1.117 Å)
(b)
1 bar
31.5 GPa
23.2 GPa
19.0 GPa
15 20 25 30 35 40 45
2θ (degrees, λ = 1.117 Å)

FIG. 2.

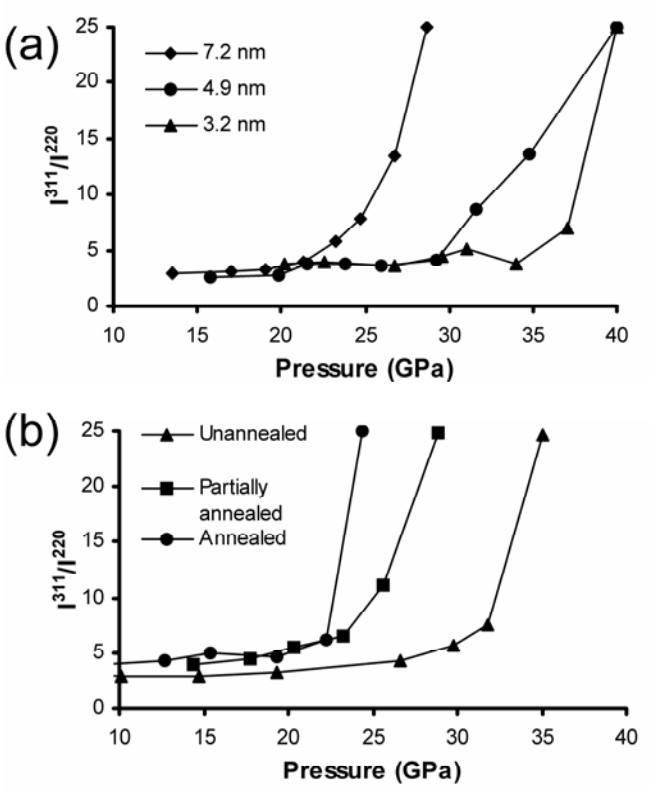
(a)
7.2 nm
4.9 nm
3.2 nm
I^{311}/I^{220}
0 5 10 15 20 25
10 15 20 25 30 35 40
Pressure (GPa)
(b)
Unannealed
Partially annealed
Annealed
I^{311}/I^{220}
0 5 10 15 20 25
10 15 20 25 30 35 40
Pressure (GPa)

FIG. 3.

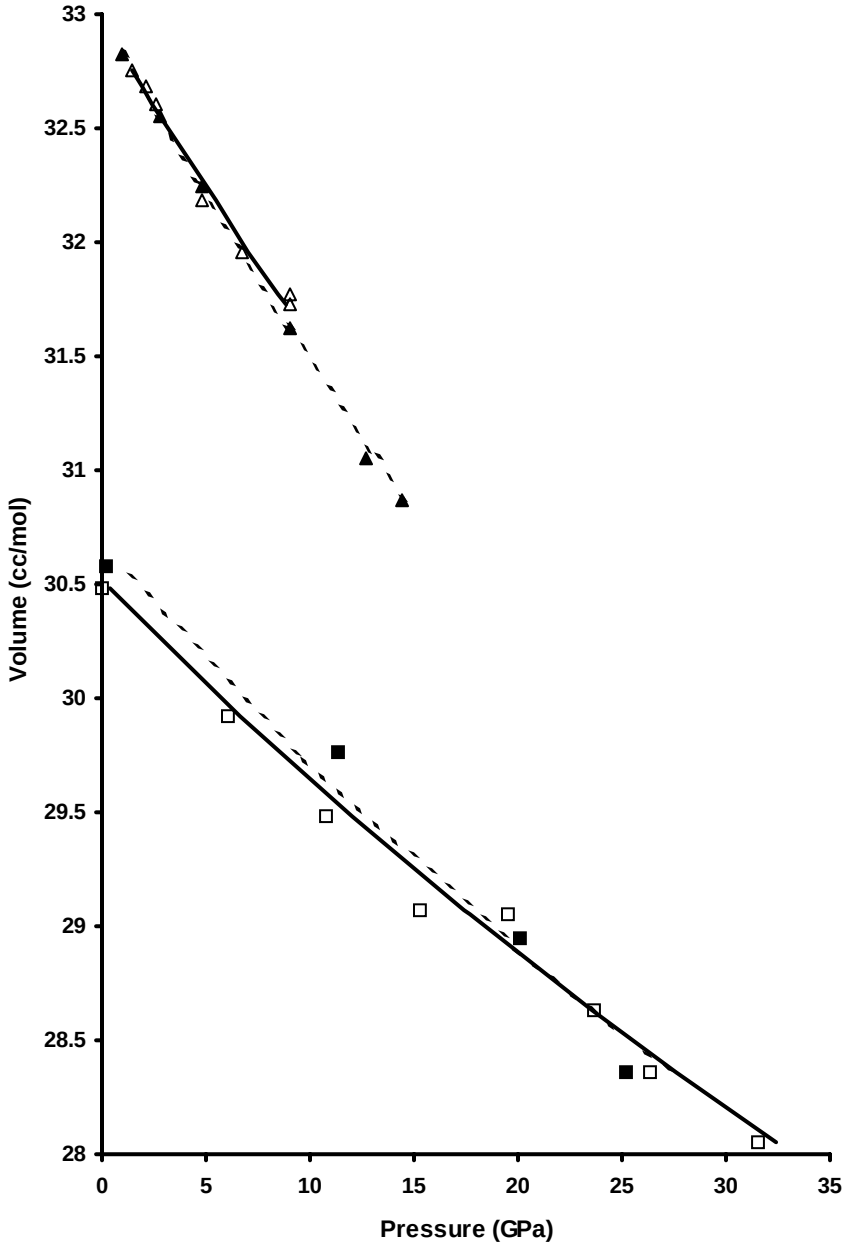
33
32.5
32
31.5
31
30.5
30
29.5
29
28.5
28
Volume (cc/mol)
0
5
10
15
20
25
30
35
Pressure (GPa)

FIG. 4.

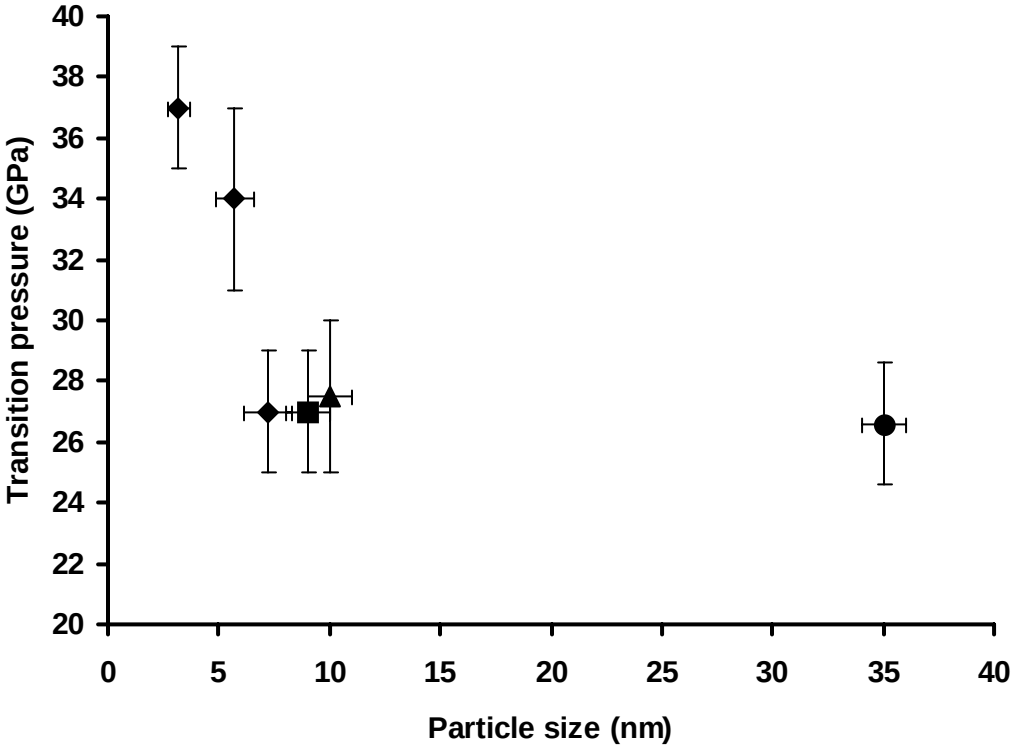
Transition pressure (GPa)
40
38
36
34
32
30
28
26
24
22
20
0
5
10
15
20
25
30
35
40
Particle size (nm)

FIG. 5.

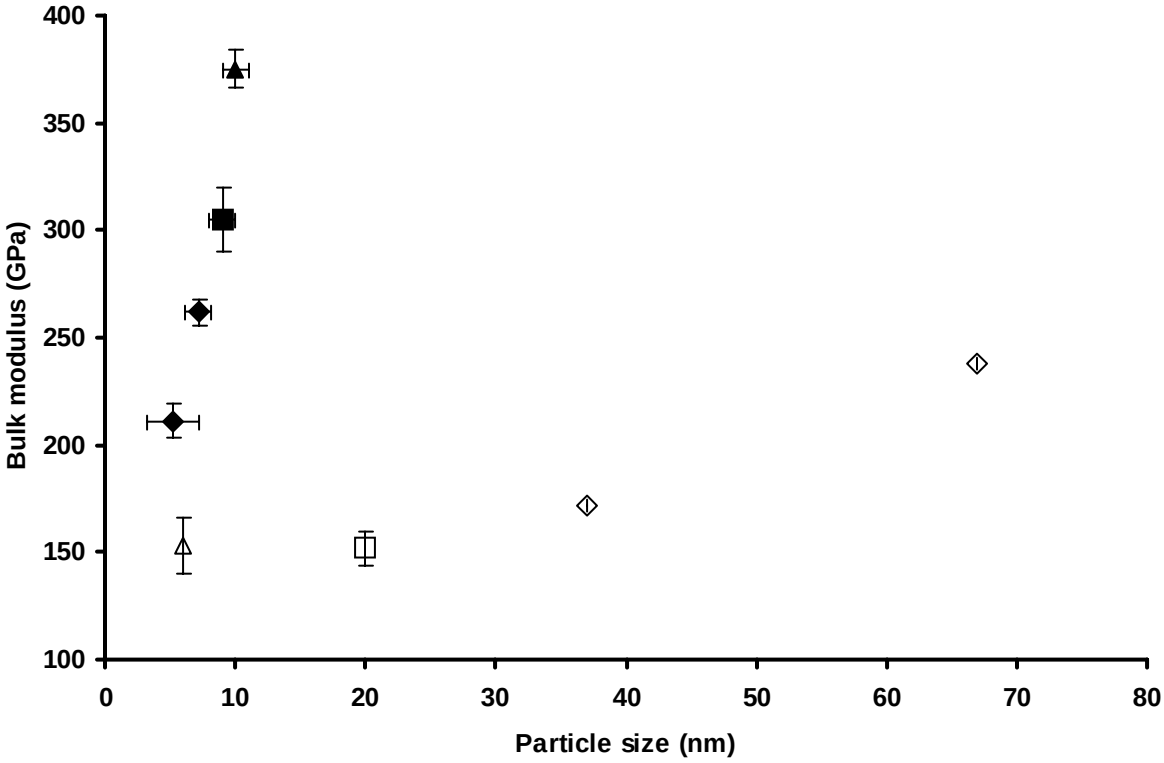
Bulk modulus (GPa)
400
350
300
250
200
150
100
0
10
20
30
40
50
60
70
80
Particle size (nm)